All-fiber passively mode-locked Tm-doped NOLM-based oscillator operating at 2-μm in both soliton and noisy-pulse regimes

Jianfeng Li,[1,2,*] Zuxing Zhang,[1] Zhongyuan Sun,[1] Hongyu Luo,[2] Yong Liu,[2] Zhijun Yan,[1] Chengbo Mou,[1] Lin Zhang,[1] and Sergei K. Turitsyn[1]

[1]*Aston Institute of Photonic Technologies (AIPT), Aston University, Birmingham, UK*
[2]*State Key Laboratory of Electronic Thin Films and Integrated Devices, School of Optoelectronic Information, University of Electronic Science and Technology of China (UESTC), Chengdu 610054, China*
[*]*lijianfeng@uestc.edu.cn*

Abstract: A self-starting all-fiber passively mode-locked Tm^{3+}-doped fiber laser based on nonlinear loop mirror (NOLM) is demonstrated. Stable soliton pulses centered at 2017.33 nm with 1.56 nm FWHM were produced at a repetition rate of 1.514 MHz with pulse duration of 2.8 ps and pulse energy of 83.8 pJ. As increased pump power, the oscillator can also operate at noise-like (NL) regime. Stable NL pulses with coherence spike width of 341 fs and pulse energy of up to 249.32 nJ was achieved at a center wavelength of 2017.24 nm with 21.33 nm FWHM. To the best of our knowledge, this is the first 2 μm region NOLM-based mode-locked fiber laser operating at two regimes with the highest single pulse energy for NL pulses.

OCIS codes: (140.3510) Lasers, fiber; (140.3480) Lasers, diode-pumped.

References and links

1. R. C. Sharp, D. E. Spock, N. Pan, and J. Elliot, "190-fs passively mode-locked thulium fiber laser with a low threshold," Opt. Lett. **21**(12), 881–883 (1996).
2. Q. Wang, J. Geng, T. Luo, and S. Jiang, "Mode-locked 2 mum laser with highly thulium-doped silicate fiber," Opt. Lett. **34**(23), 3616–3618 (2009).
3. Q. Wang, J. Geng, T. Luo, and S. Jiang, "2 μm mode-locked fiber laser," Proc. SPIE **8237**, 82371N (2012).
4. M. A. Solodyankin, E. D. Obraztsova, A. S. Lobach, A. I. Chernov, A. V. Tausenev, V. I. Konov, and E. M. Dianov, "Mode-locked 1.93 microm thulium fiber laser with a carbon nanotube absorber," Opt. Lett. **33**(12), 1336–1338 (2008).
5. K. Kieu and F. W. Wise, "Soliton Thulium-doped fiber laser with carbon nanotube saturable absorber," IEEE Photonics Technol. Lett. **21**(3), 128–130 (2009).
6. Q. Q. Wang, T. Chen, M. Li, B. Zhang, Y. Lu, and K. P. Chen, "All-fiber ultrafast thulium-doped fiber ring laser with dissipative soliton and noise-like output in normal dispersion by single-wall carbon nanotubes," Appl. Phys. Lett. **103**(1), 011103 (2013).
7. J. Liu, S. D. Wu, J. Xu, Q. Wang, Q. H. Yang, and P. Wang, "Mode-locked 2 μm thulium-doped fiber laser with graphene oxide saturable absorber," in *Lasers and Electro-Optics (CLEO)*, Technical Digest (Optical Society of America, 2012), paper JW2A.76.
8. M. Zhang, E. J. R. Kelleher, F. Torrisi, Z. Sun, T. Hasan, D. Popa, F. Wang, A. C. Ferrari, S. V. Popov, and J. R. Taylor, "Tm-doped fiber laser mode-locked by graphene-polymer composite," Opt. Express **20**(22), 25077–25084 (2012).
9. B. Fu, L. L. Gui, X. Li, X. S. Xiao, H. W. Zhu, and C. X. Yang, "Generation of 35-nJ nanosecond pulse from a passively mode-locked Tm, Ho-codoped fiber laser with graphene saturable absorber," IEEE Photonics Technol. Lett. **25**(15), 1447–1449 (2013).
10. L. E. Nelson, E. P. Ippen, and H. A. Haus, "Broadly tunable sub-500 fs pulses from an additive-pulse mode-locked thulium-doped fiber ring laser," Appl. Phys. Lett. **67**(1), 19–21 (1995).
11. Q. Wang, T. Chen, B. Zhang, A. P. Heberle, and K. P. Chen, "All-fiber passively mode-locked thulium-doped fiber ring oscillator operated at solitary and noiselike modes," Opt. Lett. **36**(19), 3750–3752 (2011).
12. X. He, A. Luo, Q. Yang, T. Yang, X. Yuan, S. Xu, Q. Qian, D. Chen, Z. Luo, W. Xu, and Z. Yang, "60 nm bandwidth, 17 nJ noiselike pulse generation from a thulium-doped fiber ring laser," Appl. Phys. Express **6**(11), 112702 (2013).

13. M. A. Chernysheva, A. A. Krylov, P. G. Kryukov, N. R. Arutyunyan, A. S. Pozharov, E. D. Obraztsova, and E. M. Dianov, "Thulium-doped mode-locked all-fiber laser based on NALM and carbon nanotube saturable absorber," Opt. Express **20**(26), B124–B130 (2012).
14. M. A. Chernysheva, A. A. Krylov, P. G. Kryukov, and E. M. Dianov, "Nonlinear amplifying loop-mirror-based mode-locked thulium-doped fiber laser," IEEE Photonics Technol. Lett. **24**(14), 1254–1256 (2012).
15. M. A. Chernysheva, A. Krylov, C. Mou, R. Arif, A. Rozhin, M. H. Rümmeli, S. Turitsyn, and E. M. Dianov, "300-mW average output power hybrid mode-locked thulium-doped fiber laser," in *Proc. ECOC* (2013), paper P.1.9.
16. C. W. Rudy, M. J. F. Digonnet, and R. L. Byer, "Thulium-doped germanosilicate mode-locked fiber lasers," in *Fiber Laser Applications (FILAS)*, Lasers, Sources, and Related Photonic Devices Technical Digest (Optical Society of America, 2012), FTh4A.
17. C. W. Rudy, K. E. Urbanek, M. J. F. Digonnet, and R. L. Byer, "Amplified 2-μm thulium-ooped all-fiber mode-locked figure-eight laser," J. Lightwave Technol. **31**(11), 1809–1812 (2013).
18. Q. Wang, J. H. Geng, Z. Jiang, T. Luo, and S. B. Jiang, "Mode-locked Tm–Ho-codoped fiber laser at 2.06 μm," IEEE Photonics Technol. Lett. **23**(11), 682–684 (2011).
19. G. P. Agrawal, *Nonlinear Fiber Optics*, 4th ed. (Academic, 2007).
20. L. Zhang, A. R. El-Damak, Y. Feng, and X. Gu, "Experimental and numerical studies of mode-locked fiber laser with large normal and anomalous dispersion," Opt. Express **21**(10), 12014–12021 (2013).
21. L. M. Zhao and D. Y. Tang, "Generation of 15-nJ bunched noise-like pulses with 93-nm bandwidth in an erbium-doped fiber ring laser," Appl. Phys. B **83**(4), 553–557 (2006).
22. M. Horowitz, Y. Barad, and Y. Silberberg, "Noiselike pulses with a broadband spectrum generated from an erbium-doped fiber laser," Opt. Lett. **22**(11), 799–801 (1997).
23. O. Pottiez, R. Grajales-Coutiño, B. Ibarra-Escamilla, E. A. Kuzin, and J. C. Hernández-García, "Adjustable noiselike pulses from a figure-eight fiber laser," Appl. Opt. **50**(25), E24–E31 (2011).
24. S. Lin, S. Hwang, and J. Liu, "Supercontinuum generation in highly nonlinear fibers using amplified noise-like optical pulses," Opt. Express **22**(4), 4152–4160 (2014).
25. A. Zaytsev, C. H. Lin, Y. J. You, C. C. Chung, C. L. Wang, and C. L. Pan, "Supercontinuum generation by noise-like pulses transmitted through normally dispersive standard single-mode fibers," Opt. Express **21**(13), 16056–16062 (2013).
26. S. K. Turitsyn, B. Bale, and M. P. Fedoruk, "Dispersion-managed solitons in fibre systems and lasers," Phys. Rep. **521**(4), 135–203 (2012).
27. B. Bale, O. G. Okhotnikov, and S. K. Turitsyn, "Modeling and technologies of ultrafast fiber lasers," in *Fiber Lasers* (Wiley-VCH, 2012).

1. Introduction

Pulsed Tm^{3+}-doped fiber (TDF) lasers operating at 2 μm eye-safe spectral region have attracted substantial attention because of their potential applications in metrology, remote sensing, free-space communication, time-resolved molecular spectroscopy, and mid-IR supercontinuum generation. A number of passively mode-locked TDF lasers have been already reported [1–16]. They can be roughly divided independently of the operation wavelength into two major categories depending on the mode-locking mechanism. The first group can be defined as material saturable absorber (SA) based laser, in which the real absorbing media, e.g., semiconductor saturable absorber mirror (SESAM), single-wall carbon nanotube saturable absorber (SWCNTSA) and graphene, are employed to initiate and shape the pulses. The second is referred as nonlinear switching based laser, in which the transmission or reflectivity property is dependent on the nonlinear phase shift induced by nonlinear polarization evolution (NPE), nonlinear amplifying loop mirror (NALM) or nonlinear optical loop mirror (NOLM), all exhibiting the capability of pulse self-shaping that is equivalent to a real saturable absorber (SA).

For the first category, a variety of laser schemes have been demonstrated [1–9]. Wang *et al.* reported an SESAM-based mode-locked fiber laser operating in the anomalous dispersion regime at 1980 nm with pulse duration of 1.5 ps and energy of 0.76 nJ [2]. Then, they extended the wavelength beyond 2 μm while narrowed the duration to 140 fs via extra-cavity compression [3]. Solodyankin *et al.* reported the first mode-locked ring cavity TDF laser at 1.93 μm by employing an SWCNTSA, which produced 1.32 ps soliton pulses with 3.4 mW average power [4]. Recently, a mode-locked TDF laser using an SWCNTSA with a large net normal dispersion was demonstrated which operated in both dissipative soliton and noise-like operation regimes around 1.947 μm with a pulse width and energy of 47 ps and 0.45 nJ for the

former and over 100 ps and 1.27 nJ for the latter [6]. Liu *et al.* demonstrated the first mode-locked TDF laser operating at 2.007 μm with 0.56 nJ pulse energy employing a graphene oxide [7]. A different graphene-based mode-locked TDF laser- operating at 1.94 μm in a large anomalous dispersion regime with pulse duration of 3.6 ps and energy of 0.4 nJ was also reported [8]. Recently, Fu *et al.* have reported a passively mode-locked Tm-Ho-codoped fiber laser based on graphene operating with the highest reported pulse energy of up to 35 nJ at 1896.69 nm, however, the peak power was very low due to its long pulse width of over 100 ns [9].

For the second category, Nelson *et al.* presented the first mode-locked TDF laser operating in the soliton regime based on NPE [10]. Recently, Wang *et al* have reported a 1.97 μm all-fiber mode-locked TDF laser with NPE which can operate at both soliton and noise-like pulse (NLP) regimes [11]. He *et al*. have reported an NPE based all-fiber mode-locked TDF laser operating at NLP regimes with a spectrum width of 60 nm and pulse energy of 17 nJ [12]. Chernysheva *et al.* have combined NALM and SWCNT to realize a hybrid mode-locked TDF laser with a pulse width of 450 fs and a maximum average power of 18 mW, and also demonstrated the different operation regimes by dispersion management [13]. Then, they combined NALM and SESAM to realize a mode-locked TDF laser with a pulse width of sub-300 fs and a maximum power of 108 mW [14]. Recently, they combined NPR and SWCNT to realize hybrid mode-locked pulses with 600 fs and 1.28 ps duration, respectively [15]. Rudy *et al.* have reported an NALM-based "figure-of-eight" mode-locked TDF laser with a pulse width of 685 fs and pulse energy of 8.75 nJ using some C band fiber components [16]. Furthermore, by improving the setup with new 2 μm components, they have recently demonstrated the first "figure-of-eight" mode-locked double-clad TDF laser with an NALM, which operated at solitary regime with a pulse width of 1.5 ps and pulse energy of 63 pJ. However, its slope efficiency was only 0.2% due to high loss in the cavity [17].

In this paper, we report the demonstration of a 2.0-μm all-fiber mode-locked double-clad TDF laser with the NOLM structure and large net anomalous dispersion which can operate at both solitary and NLP regimes. 2.8 ps soliton pulses with pulse energy of 83.8 pJ and SNR of ~62 dB, and 341 fs noisy double-scale pulses with pulse energy of 249 nJ and SNR of ~60 dB were achieved, respectively.

2. Experiment setup and results

The experimental arrangement for the "figure-of-eight" mode-locked double-clad TDF based on NOLM is shown in Fig. 1. The left loop is a ring oscillator and the right one is the nonlinear loop mirror. The active fiber in the ring oscillator is double-clad Tm^{3+}-doped fiber (Coractive, DCF-TM-10/128) with an octagonal shaped pump inner cladding with a diameter of 128 μm and a numerical aperture (NA) of 0.45. The fiber core has a 10 μm diameter with a NA of 0.22. The Tm^{3+} dopant concentration in the fiber core is about 5 wt. % and the measured absorption at 793 nm is ~4.0 dB/m. The selected fiber length of 7.0 m provides >98% pump absorption efficiency.

Two 793 nm diode lasers (Lumics, German) were used to pump the Tm^{3+}-doped fiber through a (2 + 1) × 1 pump combiner (ITF, Canada). The maximum launched pump power was 7.56 W. An isolator with an insertion loss of 0.85 dB and an extinction ratio of 35 dB at 2.02 μm (AFR) was inserted in the ring oscillator to ensure the unidirectional laser operation. A 2 × 2 fused fiber coupler coupled the left loop to the right NOLM. This coupler centered at 2.02 μm with an insertion loss of 0.62 dB provides a coupling ratio of 55:45 over 40 nm bandwidth. Note that the coupling ratio chosen as 55:45 instead of 50:50 is to increase the nonlinear phase shift difference between the clockwise and anti-clockwise directions. In addition, the slight difference in coupling ratio makes the NOLM operating at an efficient intensity-dependent "on-off" state to ensure the pulses from two directions can be interfered with maximum contrast. The SM2000 fiber (Thorlabs, USA) designed for 2 μm operation with a cut-off wavelength at 1.7 μm was chosen as the passive fiber in the NOLM for the merit of its relatively

low background loss and bend loss around 2 μm compared to SMF-28e and SMF-28e + fiber. The length of SM2000 fiber was optimized to 130 m to ensure enough nonlinear phase shift difference for stable mode-locking through the NOLM. Two polarization controllers (PC1 and PC2) were placed close to the 55:45 coupler in the NOLM to strengthen the nonlinear phase shift difference through the accumulated NPR effect and initiate mode-locking as well. The pulses are coupled out of the oscillator using a 10:90 coupler with an insertion loss of 1.1 dB at 2.015 μm.

The length of total cavity is about 132 m including 7 m TDF, 120 m SM2000 fiber and 5 m SMF-28e pigtail fiber from the pump combiner, isolator and couplers. The anomalous dispersion values of the TDF and the SM2000 fiber at 2.02 μm were about −91 ps^2/km and −100 ps^2/km respectively, which are provided by the fiber producer. The dispersion of the SMF-28e at 2.02 μm was estimated to be −91 ps^2/km according to the measured dispersion value at 1.9 μm [3]. The small amount of dispersion due to the optical isolator can be neglected. Thus, the net dispersion in the cavity was estimated to be ~−13.09 ps^2, suggesting that the laser was operating at a significantly large anomalous dispersion regime. For the measurements of the laser output, an InGaAs photodetector (EOT ET-5000F, USA) with a response time of approximately 28 ps connected to a 2.5 GHz digital oscilloscope was used to measure the pulse train and pulse waveforms. The pulse duration was measured by an interference autocorrelator (APE, German). The spectrum of pulse was measure by an OSA (Yokogawa AQ6375, Japan).

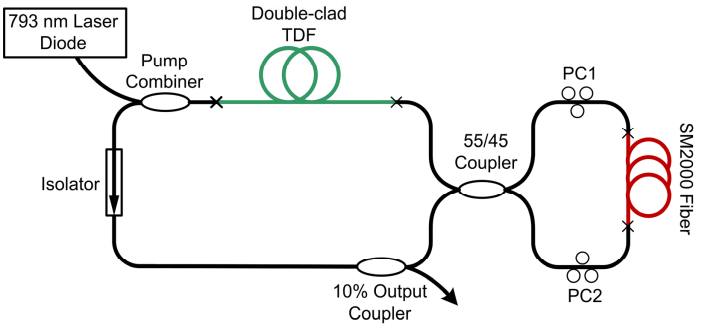

Fig. 1. Schematic of the "figure-of-eight" mode-locked double-clad TDF laser based on NOLM.

The oscillator started to operate at continuous wave (CW) regime after reaching the launched pump power of 1.328 W. Operation in this regime occurred with a small pump power range. Stable self-starting mode-locked pulses were observed as shown in Fig. 2(a) by carefully adjusting the polarization controllers (PCs) when the launched pump power was increased to 1.334 W. The measured repetition rate of 1.514 MHz matches well with the cavity length dependent theoretically value suggesting that the oscillators operates with a single pulse per round trip. The average output power at was measured to be 64 μW and the pulse energy was calculated to be 42.3 pJ. Once the mode locking achieved by the initial adjustment of the polarization controllers, the soliton pulses were self-starting and no longer needed to adjust the PCs, even for increased and re-switched pump power. It worth mentioning that the performance of soliton mode-locking was significantly sensitive to the position of the PCs. Slight adjustment of the PCs from their optimized positions would lead to CW breakthrough because of the existence of CW path in the oscillator induced by the coupling ratio of 55:45. Fortunately, the PCs enabled polarization dependent loss of the coupler to compensate the deviation from 50% thus close the CW path. The mode locking state could then be maintained to the launched pump power of 1.338 W, which gives a maximum output power of 127 μW and pulse energy of 83.8 pJ.

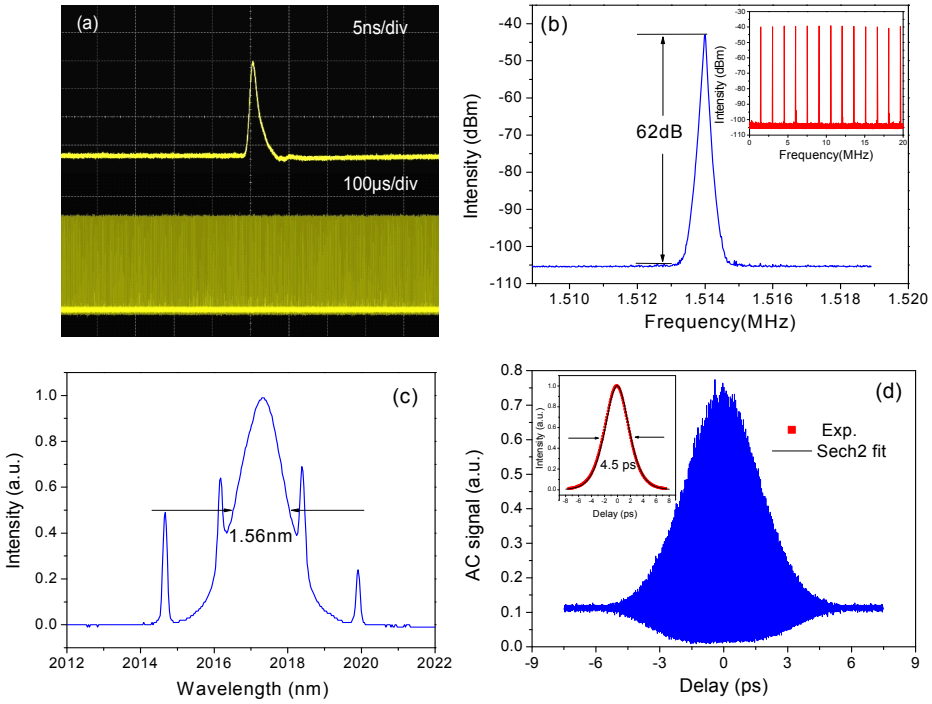

Fig. 2. Fiber oscillator under solitary operation: (a) waveform and sequence on oscilloscope; (b) RF spectrums with scanning range of 10 kHz and 20 MHz (inset); (c) optical spectrum; (d) interference and intensity autocorrelation with sech^2-pulse fitting (inset).

Figure 2(b) shows the RF spectrum of the output at a scanning range of 10 kHz with a resolution of 100 Hz at the launched pump power of 1.338 W. The signal noise ratio (SNR) of ~62 dB and the absence of modulation in 20 MHz broad RF spectrum [see inset of Fig. 2(b)] indicated that the oscillator operated at stable CW mode-locking regime. The smooth noise floor also indicated that the oscillator operated with low amplitude noise. Figure 2(c) shows the measured optical spectrum of the soliton pulses at the launched pump power of 1.338 W with a resolution of 0.02 nm. The central wavelength and FWHM were 2017.33 nm and 1.56 nm, respectively. Typical Kelly sidebands originating from spectral interference of dispersive waves suggested the operation in this case was the conventional solitary mode-locking. The separations of the peaks of first-order and second-order Kelly sidebands from the main lobe were 1.10 nm and 2.62 nm, respectively. Except for Kelly sidebands, the absence of additional narrow spectral line confirms that the pulses are free of CW components. Note that CW break-through generally started with the Kelly sideband if the PCs shifted from the optimum positions. Figure 2(d) shows the measured interference autocorrelation trace of the mode-locked pulses at a scanning range of 15 ps. The shoulder to peak ratio is 1:8 confirming that the oscillator operated at typical solitary mode-locking regime as well. The intensity autocorrelation which is independent of phase modulation type was extracted from the interference autocorrelation data using Fourier filtering algorithm integrated in the software, as shown in the inset of Fig. 2(d). The full width at half maximum (FWHM) is 4.5 ps. The experiment date was fitted by a sech^2-pulse profile very well, and the pulse duration was estimated to be 2.8 ps. Consequently, the time-bandwidth time (TBP) was calculated to be 0.324 indicating the pulse is almost transform-limited. The limited soliton pulse energy before pulse breaking or multi-pulsing occurring was calculated according to the formula given in [18], i.e., $E_{max} = 3.11\lambda^2 |D_{ave}| /(2\pi c\gamma\tau_{FWHM})$. In our case, the center wavelength λ and pulse width τ were measured to be 2017.33 nm and 2.8 ps, respectively. The average dispersion of the ring

cavity D_{ave} was roughly calculated to be 45.96 ps/nm/km. The nonlinear coefficient γ could be also calculated as 0.44 W^{-1} km^{-1} using the typical formula in [19] while assuming the nonlinear refractive index was 2.2×10^{-20} m^2/W. The calculated limited soliton pulse energy was ~0.25 nJ, and thus the limited output energy of 25 pJ was lower than the experiment result. We also used this formula to test the measured results in Ref [11]. and Ref [17], respectively. The calculated limited output energy of 37 pJ and 29 pJ were much lower than the measured 150 pJ and 79 pJ, respectively. Further increasing the pump power, soliton splitting initially appeared in temporal domain due to energy overflow of single soliton pulse. Thereafter, the multi-pulsing operation regime was terminated by the CW oscillation started from the Kelly sidebands once the launched pump power reached 1.382 W.

As the launched pump power increased to 1.68 W, the oscillator was switched to a stable mode-locked NL regime by adjusting the PCs, as shown in Fig. 3(a). At this launched pump power, the average output power was 21.1 mW. Also, once the mode locking was started by the initial tuning of the polarization, the pulses were self-starting and did not need tuning the polarization when the pump power was switched on and increased. The NL mode-locking state can be maintained to the maximum launched pump power of 7.56 W with an average output power of 377.3 mW. Note that the mode-locking also could be maintained if we decreased the launched pump power to 1.42 W owing to the higher peak power at lower average power compared to CW laser sustaining the nonlinear switching function of NOLM. In all of the pump power range, the laser always emitted single pulse, no pulse breaking or multiple pulse operation was observed as confirmed with the oscilloscope together with the autocorrelation trace measurement. Figure 3(b) demonstrates the RF spectrum at a scanning range 10 kHz with a resolution of 100 Hz at this launched pump power of 1.68 W. The measured repetition rate of 1.514 MHz as soliton pulses indicated that the oscillator operated at the fundamental mode-locking regime. The SNR of ~60 dB was similar as that of NL pulses at 2 μm region with large anomalous dispersion [12] and larger than typical 40~50 dB of NL pulses at 1.0 and 1.5 μm regions [20, 21], which indicated the low-amplitude noise of inner pulses in the noise-like packet. No side lobes were observed in the RF spectrum which are always obvious in the NL regime [6, 19, 20] suggesting the absence of appreciable fluctuations of pulse duration. The SNR was essentially unchanged with the increasing pump power. Given the achieved highest average power of 377.3 mW, the maximum achieved single pulse energy can be calculated as high as 249.32 nJ. Similarly, the RF spectrum at a range of 20 MHz with a resolution of 1 kHz was free of modulation indicating no Q-switching instability. Figure 3(c) shows the measured optical spectrum of the NL pulses with a resolution of 0.02 nm at the launched pump power 1.68 W. The smooth spectrum had a typical shape of NL pulses at 1.5 and 1.9 μm regions [11, 12, 22, 23]. The center wavelength and FWHM were 2016.16 nm and 20.70 nm, respectively. Gradually increasing the pump power to maximum, the spectral profile was essentially unchanged but the center wavelength red-shifted slightly to 2017.24 nm and the FWHM increased slightly to 21.33 nm. Such wide spectrum spanning was the typical feature of mode-locked pulses operating at NL regime. Figure 3(d) shows the measured interference autocorrelation trace at a scanning range of 4.0 ps, which provides a FWHM of 498 fs. If a Gaussian-pulse profile is assumed, the width of the coherent spike is 341 fs. Note that the shoulder to peak exhibits a 1:4 ratio instead of typical 1:8 for the solitary mode-locking suggesting that there were a bunch of pulses with varying width and power overlapped in a large time scale [11]. We also used 150 ps long scanning range to measure the NL pulses. As shown in Fig. 4, a narrow spike riding on a broad pedestal was observed and the intensity ratio of the pedestal to the peak was about 0.5. The wide shoulders that extended over the entire width of our measurement window suggested that the pulse duration was longer than 150 ps at launched pump power of 1.68 W. Decreasing the launched pump power to 1.42 W, the obvious narrower pedestal was observed. Although the precise measurement of pulse duration was not possible due to the limited scanning range of our autocorrelator, the FWHM pulse width of ~1.7 ns observed from the oscilloscope (limited by the bandwidth of the detection setup) at the

highest launched pump power indicates that the actual pedestal width could be less than 1.7 ns. It was also confirmed that the NL pulses did not stretched with fiber by using an external 30.0 m long SM 2000 fiber at the output port as a result of the significant initial noise of pulses conquering the fiber dispersion induced phase distortion.

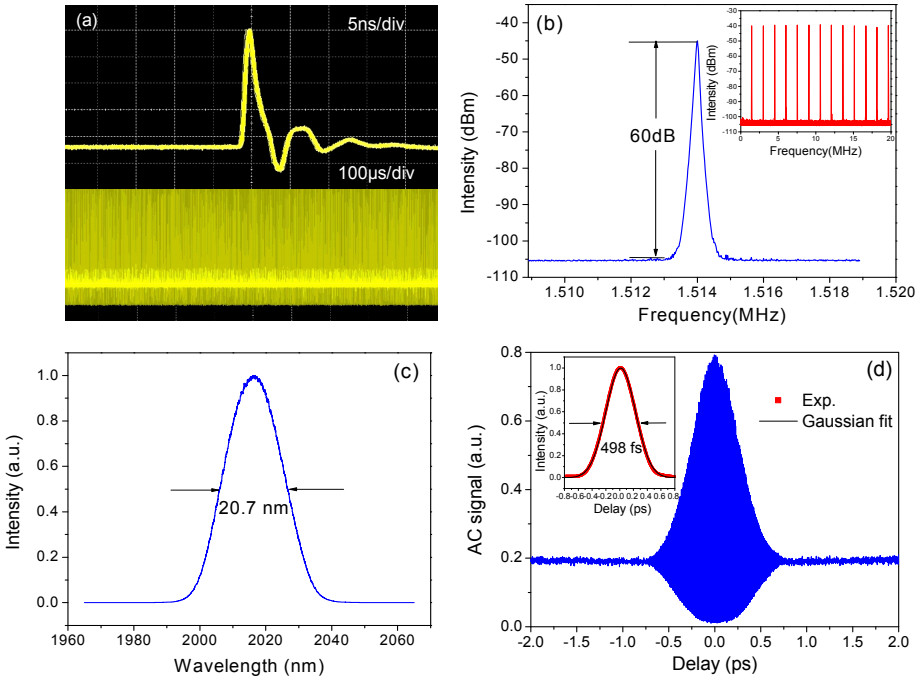

Fig. 3. Fiber oscillator under NL operation: (a) pulse waveform and sequence on oscilloscope; (b) RF spectrum with scanning range of 10 kHz and 20 MHz (inset); (c) optical spectrum; (d) interference autocorrelation and intensity autocorrelation with Gaussian-pulse fitting (inset).

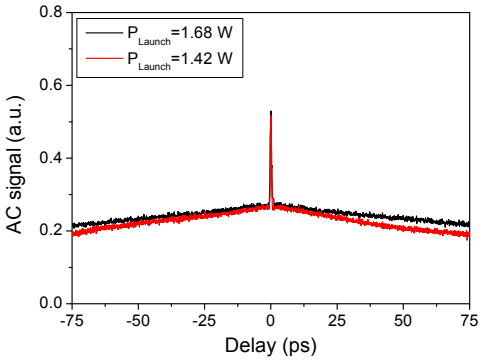

Fig. 4. Autocorrelation trace of the noise-like pulse at launched pump power of 1.68 W and 1.42 W.

To investigate the long-term stability of the mode-locked laser, we monitored 24 hours' continuous operation for soliton and noise-like regimes under laboratory condition, respectively. We found that once the mode locking was achieved and optimized through adjusting the PCs, the oscillator can keep the mode-locking state and it was not sensitive to the environmental fluctuations. Additionally, the influences of coupling ratio of the 2 × 2 coupler and the passive fiber length on the performance of the oscillator were also investigated. If replacing the coupling ratio of 55:45 by 50:50, the soliton pulses cannot be achieved due to the

weakened nonlinear phase shift difference of counter-propagating signals, and also the threshold of NL pulses increased to 3.22 W. If using the coupling ratio of 60:40, the obtained soliton pulses were always accompanied with CW signal and CW breakthrough occurred easily as well due to the enhanced CW transmission induced by the increasing coupling difference. However, the threshold of NL pulses decreased to 1.51 W, as a result of the increasing nonlinear phase shift difference. We also replaced the previously 120 m SM2000 fiber by 100 m and 80 m SM2000 fiber, respectively. The CW operation thresholds for 100 m and 80 m fiber were decreased to 1.26 W and 1.17 W, respectively, as a result of the reduced total cavity loss. For 100 m fiber, the soliton pulses cannot be self-started by only adjusting the position of PCs due to the weakened nonlinear phase shift difference. However, the soliton pulses can be achieved by increasing the launched pump power to a value at which the multiple pulses was observed by tuning the PCs, and then slightly decreasing the launched pump power. This phenomenon can be ascribed to the enhanced nonlinear phase shift difference induced by higher peak power of multiple pulses compared to CW signal. For 80 m fiber, the soliton pulses cannot be achieved through the application of the above method due to the fact that the signal power required for starting the switching function of NOLM was beyond the soliton regime. Stable NL pulses can be achieved for both 100 m and 80 m fibers with increased threshold of 1.88 W and 2.27 W, respectively.

3. Conclusion

In summary, we have demonstrated a passively all-fiber mode-locked ring cavity oscillator based on NOLM for the first time. We observed both stable solitary and NL mode-locked pulses at all-anomalous-dispersion regime. The oscillator produced 2.8 ps soliton pulses with energy of 83.8 pJ and SNR of ~62 dB centered at 2017.33 nm with a FWHM of 1.56 nm. Owing to the employing of double-clad TDF, the achieved NL pulses centered at 2017.24 nm have duration of 341 fs and singe pulse energy of up to 249 nJ which is the highest reported pulse energy from 2 μm mode-locking fiber lasers without amplification. The measured SNR of ~60 dB suggests its higher stability compared with typical NL pulses. Although the NL pulses in most of cases were not the ideal higher energy pulses due to its broad pedestal and low SNR, the NL pulses with high SNR in this case is a great potential in producing femtosecond-level pulses with high energy that could lead to a range of applications involving laser radar, large electric field interactions with molecules, material processing and pump source of mid-IR supercontinuum generation [23, 24]. Additional possibilities for stabilization and control of nonlinear dynamics are offered by the dispersion mapping using fibers with different dispersion [25–27]. Furthermore, it worth emphasizing that compared with SA-based mode-locked fiber lasers, the nonlinear switching based NOLM, NPR or NALM structures can achieve higher energy owing to higher damage threshold without real SA and shorter pulse duration owing to almost near-zero “saturable absorption” response time. Energetic ultra-short 2 μm mode-locked pulses operating at dissipative soliton regime were also expected by developing a normal dispersion cavity based on the above nonlinear switching structures.

Acknowledgments

This work was supported by National Nature Science Foundation of China (Grant No. 61377042 and 61107037), and European Commission's Marie Curie International Incoming Fellowship (Grant No. 911333). The work was also partly supported by Key Laboratory of Science and Technology on High Energy Laser, CAEP (No. 2013005580) and Science and Technology Innovation Team of Sichuan Province (No. 2011JTD0001).